Oncogene (2012) 31, 13–26

www.nature.com/onc

ORIGINAL ARTICLE

Regulation of mitosis and taxane response by Daxx and Rassf1

S Giovinazzi[1,5], CR Lindsay[1,5], VM Morozov[1], E Escobar-Cabrera[2], MK Summers[3,6], HS Han[4], LP McIntosh[2] and AM Ishov[1]

[1]*Department of Anatomy and Cell Biology, University of Florida Shands Cancer Center, Gainesville, FL, USA;* [2]*Department of Biochemistry and Molecular Biology and Department of Chemistry, University of British Columbia, Vancouver, British Columbia, Canada;* [3]*Department of Cellular Regulation, Genentech Inc., South San Francisco, CA, USA and* [4]*H Lee Moffitt Cancer Center and Research Institute, University of South Florida College of Medicine, Tampa, FL, USA*

Current theories suggest that mitotic checkpoint proteins are essential for proper cellular response to taxanes, a widely used family of chemotherapeutic compounds. We recently showed that absence or depletion of protein Daxx increases cellular taxol (paclitaxel) resistance—a common trait of patients diagnosed with several malignancies, including breast cancer. Further investigation of Daxx-mediated taxol response revealed that Daxx is important for the proper timing of mitosis progression and cyclin B stability. Daxx interacts with mitotic checkpoint protein RAS-association domain family protein 1 (Rassf1) and partially colocalizes with this protein during mitosis. Rassf1/Daxx depletion or expression of Daxx-binding domain of Rassf1 elevates cyclin B stability and increases taxol resistance in cells and mouse xenograft models. In breast cancer patients, we observed the inverse correlation between Daxx and clinical response to taxane-based chemotherapy. These data suggest that Daxx and Rassf1 define a mitotic stress checkpoint that enables cells to exit mitosis as micronucleated cells (and eventually die) when encountered with specific mitotic stress stimuli, including taxol. Surprisingly, depletion of Daxx or Rassf1 does not change the activity of E3 ubiquitin ligase anaphase promotion complex/C in *in vitro* settings, suggesting the necessity of mitotic cellular environment for proper activation of this checkpoint. Daxx and Rassf1 may become useful predictive markers for the proper selection of patients for taxane chemotherapy.
Oncogene (2012) **31,** 13–26; doi:10.1038/onc.2011.211; published online 6 June 2011

Keywords: Daxx; Rassf1A/C; taxane chemotherapy; mitosis; SAC; APC

Correspondence: Dr AM Ishov, Department of Anatomy and Cell Biology, University of Florida Shands Cancer Center, 2033 Mowry Road, Room 358, Gainesville, FL 32610, USA.
E-mail: ishov@ufl.edu
[5]These authors contributed equally to this work.
[6]Current address: Lerner Research Institute Department of Cancer Biology, Cleveland, OH, USA.
Received 3 January 2011; revised 26 March 2011; accepted 15 April 2011; published online 6 June 2011

Introduction

Cell cycle checkpoints are necessary controls that halt cell cycle progression in response to stresses that may otherwise promote genome instability. Under physiological conditions, the spindle assembly checkpoint (SAC) ensures that during mitosis all kinetochores are stably attached to microtubules before separation of chromosomes during anaphase. Spindle toxins such as taxanes (taxol/paclitaxel and docetaxel/taxotere), nocodazole and others promote conditions of prolonged mitotic stress by binding tubulin heterodimers, thus interfere with the polymerization/depolymerization of microtubules; they are widely used as cell biology tools and as chemotherapeutic agents. Paclitaxel (taxol) is one of the most common chemotherapeutic agents used to treat human cancers (reviewed by O'Shaughnessy, 2005). However, many cancer patients are resistant or become resistant to taxol during drug administration (Bonneterre *et al*., 1999; Ravdin *et al*., 2003; Crown *et al*., 2004). Overcoming resistance to these agents would represent a major advantage in the clinical treatment of breast cancer (Aapro, 2001; Henderson *et al*., 2003).

Block of microtubule dynamics can result in the potential alteration of mitotic processes, including separation of centrosomes, microtubule attachment to kinetochores (and activation of the SAC), proper alignment and separation of chromosomes. When cells are exposed to conditions of prolonged mitotic stress in the presence of microtubule poisonous drugs, the SAC is eventually inactivated and cells can exit mitosis as micronucleated and tetraploid (Mantel *et al*., 2008; Wysong *et al*., 2009). This mitotic exit is primarily dependent on the ubiquitination and proteolysis of cyclin B and Securin, a process referred to as 'mitotic slippage' or 'mitotic catastrophe' (Brito and Rieder, 2006). The proteins and pathways that govern this slippage are insufficiently characterized. Cells that lack important SAC-related proteins like Mad2 and BubR1 experience enhanced sensitivity to spindle toxins with increased occurrence of micronucleated cells (Lee *et al*., 2004; Sudo *et al*., 2004; Niikura *et al*., 2007). To date, only few examples of inactivated mitotic checkpoint proteins are known to reduce sensitivity to taxanes, including BRCA1 (Chabalier *et al*., 2006) and Mad2 antagonist protein p31^{comet} (Xia *et al*., 2004). Recently,

we reported that the nuclear protein Daxx is involved in taxane sensitivity (Lindsay *et al*., 2007). Daxx is a highly conserved and developmentally essential nuclear protein (Michaelson *et al*., 1999a; Ishov *et al*., 2004; Lindsay *et al*., 2009). Daxx is involved in numerous cellular processes such as transcriptional regulation (Lindsay *et al*., 2008), anti-viral immunity (Saffert and Kalejta, 2008), apoptosis (Michaelson, 2000; Salomoni and Khelifi, 2006) and carcinogenesis. We previously showed that, upon taxol treatment, cells with reduced level of Daxx remain in a prolonged mitotic arrest and complete cell division after taxol removal, whereas wild-type cells exit from taxol-induced mitotic block as micronucleated cells incapable of proliferation (Lindsay *et al*., 2007). Thus, Daxx-deficient cancer cells that are exposed to taxol can survive treatment, but the mechanism remains elusive.

Taxanes affect microtubule stability, but mutations or alterations in tubulin occur very rarely in cancers (Hari *et al*., 2003a). Functional screens have been directed at finding novel targets affecting sensitivity to taxol and other compounds, but it remains unclear whether these targets have a direct role in taxol sensitization or offer prognostic value to clinicians (Swanton *et al*., 2007). The existence of a mitotic stress checkpoint(s), separate in function from the SAC, has been proposed with regard to cells that have been exposed to spindle toxins (Scolnick and Halazonetis, 2000). Thus, it is essential to identify the proteins and pathways involved in taxol sensitization/resistance because foreknowledge of these targets may prove useful for proper selection of patients for taxane-based chemotherapy. To this end, we sought to further understand the phenomenon of Daxx-dependent taxol resistance related to mitosis and to determine its importance in tumors subjected to this chemotherapy. Here, we describe the cell cycle-dependent interaction of Daxx with protein RAS-association domain family protein 1 (Rassf1) in establishing the proper cellular response to taxol.

Results

Duration of mitotic stages are affected in the absence of Daxx

Resistance to taxol was observed in human breast cancer and human larynx carcinoma HEp2 cells with experimentally reduced Daxx (Lindsay *et al*., 2007). To understand the function of Daxx in taxol response, we utilized HEp2 cells expressing control or anti-Daxx short hairpin RNAs (shRNAs) (Figure 1a). We used this model cell line as taxane-based therapy is one of treatment options in head and neck cancer (De Mulder, 1999) and given the ability of HEp2 cells to recapitulate the Daxx-dependent taxol response observed in breast cancer cell lines as shown previously (Lindsay *et al*., 2007). HEp2 cells were synchronized using a double thymidine block and released for cyclin B protein level analysis to monitor G2/M/G1 progression. Although control shRNA cells showed destruction of cyclin B by 9 h post-thymidine release, Daxx-depleted cells showed

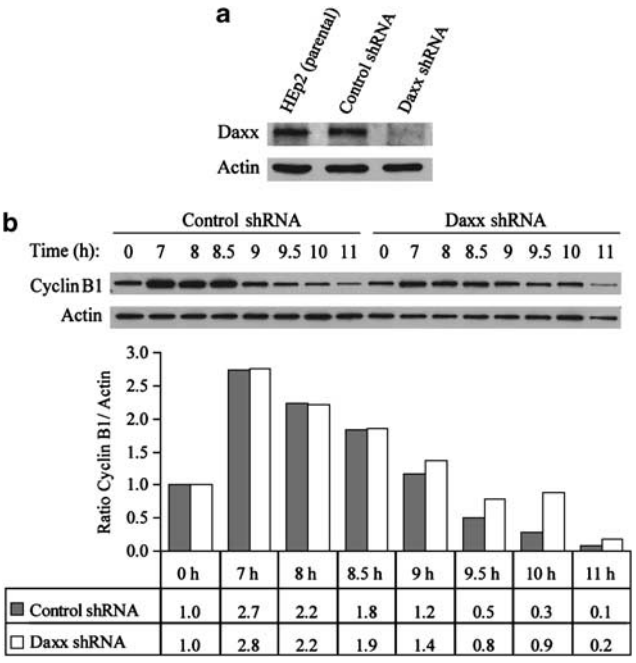

Figure 1 Daxx-dependent stability of cyclin B. (**a**) Western blot analysis of Daxx depletion in HEp2 cells. (**b**) Control- and Daxx-depleted HEp2 cells were synchronized by a double thymidine block (0 h) and then released into normal media for progression through mitosis (6–11 h). Top: Western blot analysis of cyclin B protein stability. Bottom: Relative quantization of cyclin B protein levels (normalized to actin). Cyclin B protein is stabilized longer in Daxx-depleted cells (at 9.5–11 h, post-thymidine release), indicating that Daxx-depleted cells are delayed in mitosis. Data show a representative experiment out of four.

prolonged stabilization of cyclin B at 9.5–11 h post-release, suggesting that Daxx is required for normal mitosis progression (Figure 1b).

Next, we studied mitotic progression by time-lapse microscopy in control- and Daxx-depleted cells stably transfected with histone H2B-GFP; results are summarized in Table 1. The occurrence of chromatin condensation in Daxx-depleted cells was more rapid, indicating faster progression of prophase compared with control cells (Daxx shRNA cells has average 7.5 min and control shRNA average 10.2 min). Contrarily, the average prometaphase/metaphase timing of Daxx-depleted cells (37.6 min) was longer than in control-depleted cells (average 31.2 min). No differences in mitotic progression were observed in control shRNA compared with parental HEp2 cells (data not shown). The combination of these data suggests that depletion of Daxx in human cells results in perturbation of normal mitosis, implying that Daxx is necessary for proper mitotic progression.

During interphase, Daxx is a predominately nuclear protein (Lindsay *et al*., 2009) accumulating at ND10/promyelocytic leukemia nuclear bodies (PML NBs) (Ishov *et al*., 1999), thus, we analyzed Daxx distribution throughout the cell cycle by immunofluorescent staining. As expected we found Daxx to localize predominately in the nuclei at PML NBs during interphase in mouse embryonic fibroblasts (Supplementary Figure 1, upper

Table 1 Depletion of Daxx influences mitosis stages

Stage	*shRNA*	*Average (min)*	*Standard deviation (min)*	*Min (min)*	*Max (min)*
Prophase timing	Control	10.2	2.3	6	18
	Daxx	7.5	2.64	2	14
Prometaphase–anaphase timing	Control	31.2	7.9	22	58
	Daxx	37.6	10.36	22	78

Abbreviations: Max., maximum, min., minimum; shRNA, short hairpin RNA.
Control- and Daxx-depleted HEp2 cells were stably transfected with H2B-GFP and analyzed using fluorescence time-lapse video microscopy. Duration of mitotic stages was calculated based on important morphological events associated with chromatin. Average (mean), standard deviation and min./max. values were determined for the duration of prophase and prometaphase/metaphase.

cells in both rows); however, the distribution of Daxx at PML NBs began to change during early prometaphase, when the majority of Daxx is still associated with PML NBs, and also begins to localize at spindle-like pattern (Supplementary Figure 1, upper row). By late prometaphase, the majority of Daxx is absent from PML NBs, but remains at a spindle-like pattern (Supplementary Figure 1, bottom row).

Cell cycle-dependent localization of Daxx and Rassf1

We performed a yeast two-hybrid screen to identify interacting partners that could determine Daxx-mediated mitosis progression and taxol sensitivity. Two clones corresponding to Rassf1C were identified using this method, which mapped to amino acid (aa) 5–270 and aa 30–270 of the mouse Rassf1C polypeptide (Supplementary Figure 2). Re-transformation and β-gal assay confirmed interaction of Daxx and Rassf1C clones in yeast (data not shown).

Rassf1C and Rassf1A are two major isoforms of tumor suppressor protein Rassf1; Rassf1A has been extensively studied with regard to cell cycle progression, mitosis and apoptosis (reviewed by Agathanggelou *et al*., 2005), whereas Rassf1C biology is much less understood. Previous reports addressed the interaction and function of Daxx and Rassf1. The first study described Rassf1C as a nuclear protein with Daxx-dependent accumulation at PML NBs during interphase (Kitagawa *et al*., 2006). Upon degradation of Daxx, the authors found Rassf1C to translocate into the cytoplasm where it localized to microtubules. The other report suggests that Daxx interacts with Rassf1A, although the dynamic of localization is much less understood (Song *et al*., 2008). We found that endogenous Rassf1A and Rassf1C are strictly cytoplasmic, whereas endogenous Daxx is a nuclear protein associated mostly with PML NBs (Figure 2a). In addition, the depletion of Daxx did not affect the distribution of Rassf1C/A as was previously reported by Kitagawa *et al*. (2006): it has same cytoplasmic distribution upon Daxx depletion (Figure 2a, bottom row) as in control shRNA-expressing cells (Figure 2a, top row). Biochemical fractionation of HEp2 cells into nuclear and cytosolic fractions confirmed that endogenous Rassf1 was strictly segregated into tubulin-containing (cytosolic) fractions, whereas endogenous Daxx was predominately associated with HP1-α containing nuclear fractions (Figure 2b), supporting previous data showing predominately nuclear association of Daxx (Lindsay *et al*., 2009). Confocal imaging of transiently expressed GFP-Rassf1A and GFP-Rassf1C in HEp2 cells also revealed an exclusively cytoplasmic distribution of these proteins, in contrast GFP-Daxx localization was predominately nuclear (Figure 2c); same results were obtained upon double-transfection of Daxx-GFP and Rassf1C-RFP (Figure 2d). In summary, Daxx and Rassf1 are compartmentally separated proteins during interphase: Daxx is associated with PML NBs in the nucleus, and both Rassf1 isoforms are cytoplasmic. These data confirm many previous findings of cytosolic deposition of Rassf1; Rassf1A and Rassf1C has been shown to bind tubulin, and influence microtubule dynamics (reviewed by Agathanggelou *et al*., 2005).

Being that Daxx and Rassf1 are compartmentally separated proteins during interphase, we sought to understand the dynamics of this interaction in cells by first analyzing the distribution of Daxx and Rassf1 throughout the cell cycle. Previous reports have shown that Rassf1 is a microtubule-associated protein that associates with the spindle apparatus during mitosis (Liu *et al*., 2003; Dallol *et al*., 2004; Rong *et al*., 2004) and we reasoned that the interaction between Daxx and Rassf1 may occur primarily at this time. To address this possibility, we immunostained HEp2 cells with Daxx and Rassf1 antibodies; partial colocalization between Daxx and Rassf1 was observed during prometaphase and metaphase (Figure 2e), suggesting that the primary stage of cell cycle for Daxx and Rassf1 colocalization and potential interaction is mitosis and not interphase.

Mapping of Daxx/Rassf1 interaction

As implied from yeast two-hybrid data (Supplementary Figure 2), the interaction between Daxx and Rassf1 occurs between the Rassf1C isoform and Daxx. We confirmed this interaction by *in vitro* pull-down assay (Supplementary Figure 3A). We next mapped the regions of interaction between Daxx, Rassf1C and Rassf1A using full-length or truncation mutants of these molecules in *in vitro* pull-down assay.

Human Daxx is a 740 aa protein, whereas Rassf1A and Rassf1C are 340 and 270 aa proteins, respectively

(Figure 3). Rassf1A and Rassf1C share a common 220 aa carboxyl-terminal peptide sequence that includes the microtubule-binding domain and Ras-association domain, whereas their amino-terminal regions are unique: 120 aa for Rassf1A and 50 aa for Rassf1C.

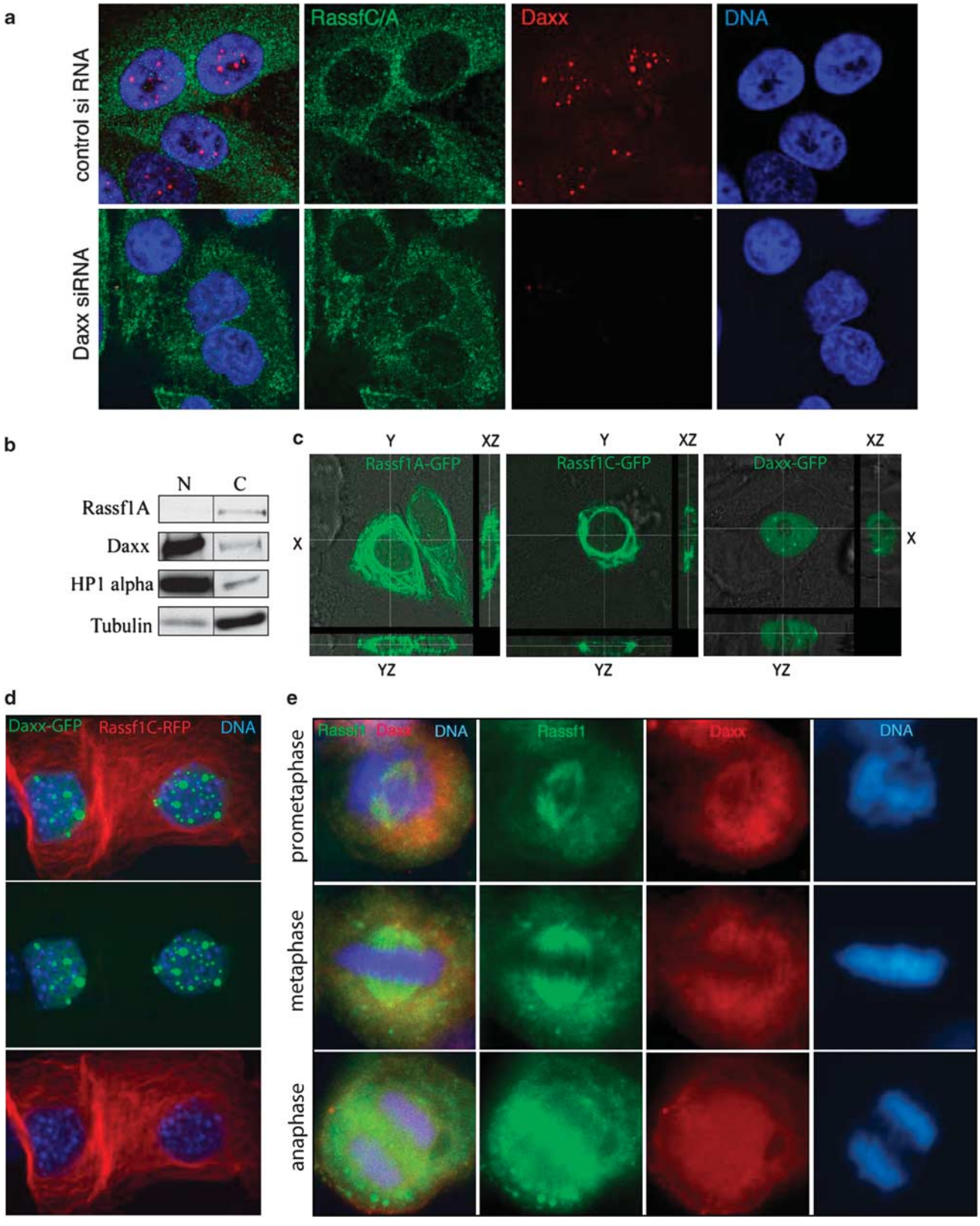

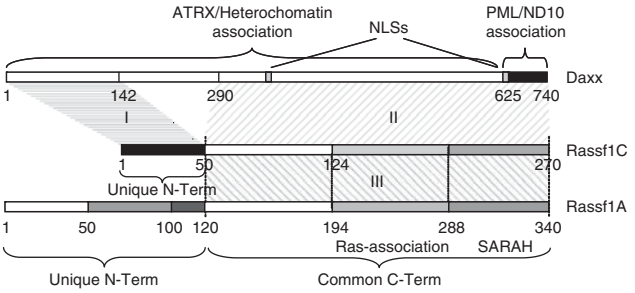

Figure 3 Mapping Daxx and Rassf1 regions of interaction. Diagram depicting human Daxx, Rassf1A and Rassf1C and their mutual regions of interaction summarizing results obtained by *in vitro* pull-down assay (Supplementary Figure 3). The first region of interaction (I) was identified between Daxx first 142 aa and Rassf1C unique N terminus. The second region of interaction (II) is mapped between Daxx C terminus (Daxx 290–740) and Rassf1C/A common region. The third region (III) involves the common region of Rassf1A and Rassf1C, indicating that the two molecules may homo- or heterodimerize via their common region.

Analysis of several truncation mutants of Daxx and Rassf1C reveals two strong regions of interaction between these proteins. The first and minimal Rassf1C-interacting region localizes among the amino terminal 142 aa, whereas the second one is mapped between aa 290 and 740 of Daxx (I and II in Figure 3 and Supplementary Figure 3). Both regions are able to bind independently to Rassf1C. The N terminus of Daxx ($Daxx^{1-142}$) binds to the unique 50 aa amino-terminal region of Rassf1C (Supplementary Figure 3B, top panel, 'I'). Daxx C-terminal region ($Daxx^{290-740}$) interacts with Rassf1C full-length and with Rassf1C/A common region ($Rassf1C^{51-270}$) (Supplementary Figure 3B, central panel, 'II'). We did not observe any specific or significant interaction of $Daxx^{290-740}$ with either of the two unique N-terminal regions of Rassf1C and Rassf1A (Supplementary Figure 3B, central panel, 'II'). We observed interaction between Rassf1 isoforms (III, Figure 3 and Supplementary Figure 3B, bottom panel), suggesting formation of homo- and heterodimers of Rassf1A/C. Thus, by *in vitro* pull-down assay we characterized two main regions of interaction between Rassf1 and Daxx and identified Rassf1A/C dimerization region (I, II and III in Figure 3). Region I was extensively mapped by NMR spectroscopy: interaction domain of Daxx includes a left-handed unique four-helix bundle (DHB domain, residues 60–137), which binds mainly to residues 28–38 of Rassf1C (Escobar-Cabrera *et al*., 2010).

Daxx- and Rassf1-depleted cells are resistant to taxol treatment

To understand the functionality of the cell cycle-dependent interaction of Daxx and Rassf1 upon taxol treatment, we produced HEp2 cells with stable expression of Rassf1A-shRNA (Figure 4a). Cells expressing control shRNA, anti-Daxx shRNA, anti-Rassf1A shRNA and parental HEp2 cells were exposed to 10 nM taxol for 12, 18 and 24 h, and then re-plated for colony formation assay. Daxx- and Rassf1A-depleted cells exhibited a strong taxol-resistant phenotype with the majority of treated cells (75–80%) capable of dividing and forming colonies after removal of taxol (Figure 4b).

Cyclin B is stabilized in Daxx- and Rassf1-depleted cells treated with Taxol

Cells with reduced Daxx display increased resistance to taxol treatment because the majority of cells arrest in mitosis for longer period of time (and thus are able to complete normal division upon taxol wash-out), whereas control cells exit mitosis towards micronucleated cells (and stop proliferation). A similar effect was previously observed upon cell exposure to low or high taxol concentrations (Lindsay *et al*., 2007). We sought to understand the taxol resistance phenomenon more in depth by analyzing the cyclin B levels in synchronized control-, Daxx- and Rassf1A-depleted cells upon 10 nM taxol treatment. Whereas cyclin B protein levels decreased by 13 h post-release in control cells, it was stabilized in Daxx- and Rassf1A-depleted cells (Figure 4c). Stabilized cyclin B upon Daxx or Rassf1A depletion is a biochemical indication of cells arrested in mitosis, whereas control cells exit mitosis by micronucleation, as confirmed morphologically for Daxx-depleted cells (Lindsay *et al*., 2007).

Expression Daxx binding motif of Rassf1C increases taxol resistance

To probe directly the functionality of Daxx–Rassf1 interaction in relation to taxol exposure, we used the interaction mapping information described in Figure 3 and Supplementary Figure 3B. We designed a minimal Rassf1C mutant for stable overexpression in cells that

Figure 2 Cell cycle-dependent localization of Rassf1 C/A and Daxx. (**a**) Rassf1C/A and Daxx localization during interphase. Control- (top) and Daxx-depleted (bottom) HEp2 cells were immunostained for Rassf1C/A (green) and Daxx (red); DNA (blue) for nuclear visualization. Note nuclear localization of Daxx in PML NBs (top). Cytoplasmic localization of Rassf1C/A is unaltered upon Daxx depletion (bottom). (**b**) Biochemical fractionation of cells shows differential localization of Daxx/Rassf1 proteins. HEp2 cells were separated into nuclear (N) and cytosolic (C) fractions. Daxx is found in HP1-α containing nuclear fractions, whereas Rassf1 is found in tubulin-containing cytoplasmic fractions. (**c**) Distribution of GFP-Rassf1A, GFP-Rassf1C and GFP-Daxx in HEp2 cells. GFP-Rassf1A (left), -Rassf1C (middle) and -Daxx (right) were transiently transfected into HEp2 cells and then analyzed by confocal microscopy. Note that distribution of both Rassf1 isoforms (Rassf1A and Rassf1C) is exclusively cytoplasmic (compare *XY*, *XZ* and *YZ* planes), whereas, in contrast, the distribution of Daxx is exclusively nuclear. (**d**) Distribution of Daxx-GFP and Rassf1C-RFP upon double transfection in HEp2 cells. Daxx-GFP is nuclear mostly accumulating in domains (PML NBs), whereas Rassf1C is cytoplasmic. (**e**) Partial colocalization of Daxx and Rassf1 during mitotic stages. HEp2 cells were immunostained with Rassf1C/A ab (green) and Daxx (red).

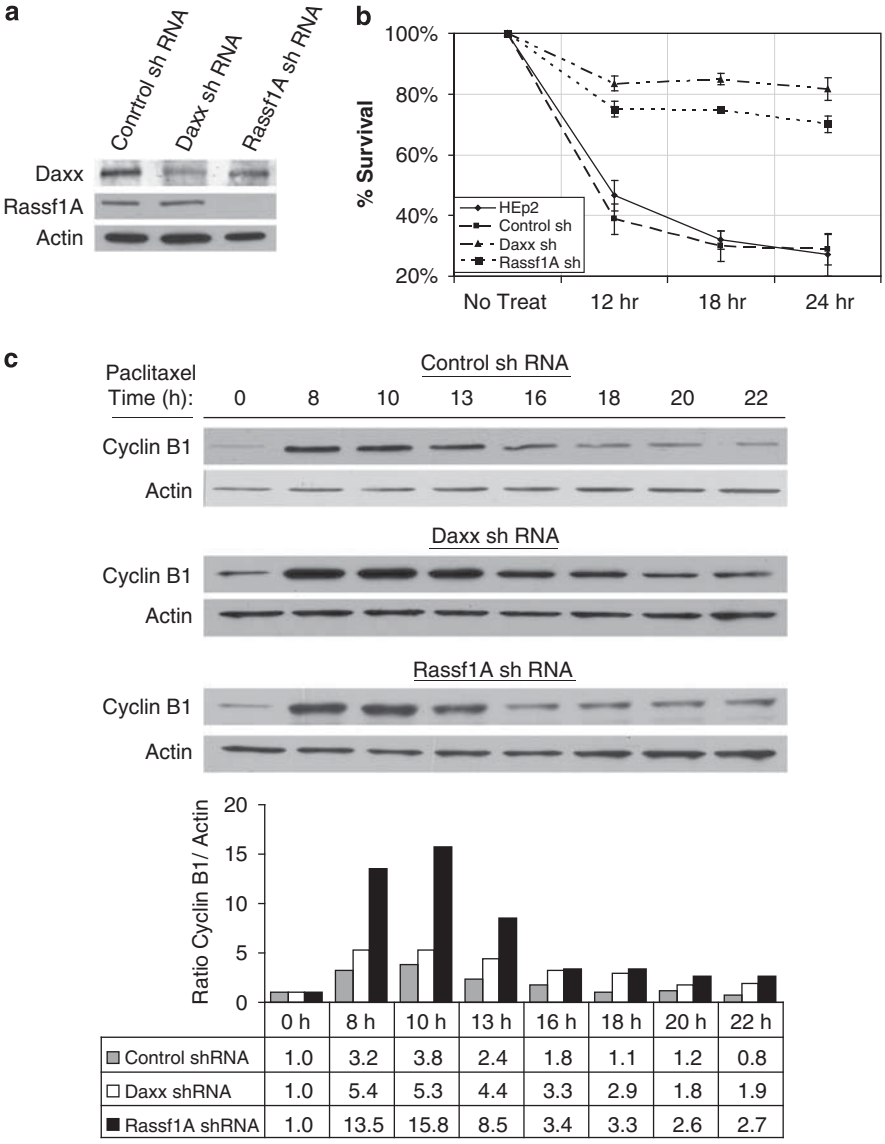

	0 h	8 h	10 h	13 h	16 h	18 h	20 h	22 h
Control shRNA	1.0	3.2	3.8	2.4	1.8	1.1	1.2	0.8
Daxx shRNA	1.0	5.4	5.3	4.4	3.3	2.9	1.8	1.9
Rassf1A shRNA	1.0	13.5	15.8	8.5	3.4	3.3	2.6	2.7

Figure 4 Depletion of Daxx or Rassf1 increases taxol resistance and prolongs cyclin B stability. (**a**) Western blot analysis of Daxx and Rassf1A depletion in HEp2 cells. (**b**) Colony formation assay of parental, control- Daxx- and Rassf1A-depleted cells exposed to 10 nM taxol for 12, 18 and 24 h after release from double thymidine block. Rapid decrease in survival is seen in parental and control cells, whereas Daxx- and Rassf1A-depleted cells withstood taxol treatment and produced colonies. (**c**) Western blot analysis of cyclin B protein stability in HEp2 control-, Daxx- and Rassf1A-siRNA cell lines treated with taxol for the indicated amount of time (6–22 h). Cells were synchronized using a double thymidine block and released (0 h) into normal media containing 10 nM taxol. The bottom panel: densitometry analysis of cyclin B normalized by actin; for each cell line, the cyclin B/actin ratio at 0 h set as 1.0. Whereas cyclin B protein levels rapidly decrease by 13 h post-thymidine release in control shRNA cells, cyclin B protein levels were stabilized longer in Daxx- and Rassf1A-depleted cells (through 22 h, post-thymidine release), indicating that Daxx and Rassf1A depletion prolongs exit from mitosis in response to taxol exposure. Data show a representative experiment out of three.

(1) retains its Daxx-binding ability and (2) potentially interferes with Daxx–Rassf1C interaction, perturbing taxol sensitization. We expressed GFP-Rassf1C aa 1–50 and GFP in HEp2 cells (Figure 5a for expression) and then treated these stable-expressing cell lines along with parental HEp2 cells with 10 nM taxol and re-plated them for colony formation assay. In the case of the GFP-Rassf1C 1–50 cell line, we observed an overall increase in survival after taxol exposure compared with controls (Figure 5b). This suggested that Rassf1C 1–50-expressing cells could survive taxol treatment due to prevention of mitotic slippage towards micronucleation, brought upon by potential disruption of Daxx–Rassf1C binding.

Analysis of mitosis-related proteins upon Daxx depletion

Daxx exhibits transcription repression activity (reviewed by Lindsay *et al*., 2008); thus, it could potentially regulate mitotic progression and taxol sensitivity repressing mitotic checkpoint proteins. In this regard, Daxx depletion does not change accumulation of several mitosis-related proteins including Cdc27, Cdc20 and

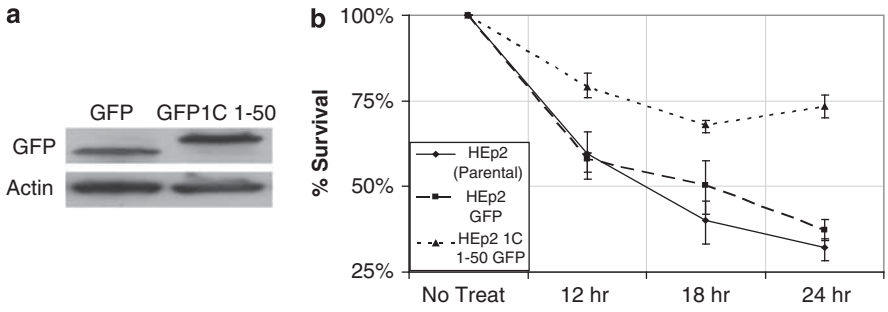

Figure 5 Expression of Daxx binding motif of Rassf1C leads to increased taxol resistance. (**a**) Western blot characterization of GFP and GFP-Rassf1C 1–50 aa expressing HEp2 cell lines. (**b**) Expression of Rassf1C 1–50 (but not GFP alone) leads to increased taxol resistance (treatment with 10 nM taxol for indicated time) relative to parental HEp2 cells by colony formation assay.

Mad2 (Supplementary Figure 4A). No cell cycle-specific changes of Daxx protein level were observed either (Supplementary Figure 4B). The combination of these data may suggest that Daxx-mediated taxol sensitivity is independent of the previously reported transcription repression activity of Daxx, at least for tested SAC-related proteins, and more likely is dependent on the function of a Daxx/Rassf1-specific interaction.

Rassf1A or Daxx are not required for activation of the anaphase promotion complex in vitro

To determine whether Rassf1A or Daxx were required for the activity of mitotic E3 ubiquitin ligase anaphase promotion complex (APC)/C or release from the spindle checkpoint, we utilized an *in vitro* system using mitotic extracts, which recapitulates both of these activities (Summers *et al*., 2008). APC activity was determined by monitoring the destruction of radio-labeled Securin, which remained stable throughout all extracts derived from cells (control-, Daxx- or Rassf1A-depleted) and confirmed an active spindle checkpoint (Supplementary Figure 5A). During the incubation, extracts undergo a slow spontaneous release from spindle checkpoint-mediated inhibition. The loss of neither Rassf1A nor Daxx did not delay the kinetics of this release, suggesting that they are not required for direct activation of the APC upon checkpoint silencing. We tested this idea directly, by asking whether the Mad2 antagonist, $p31^{comet}$, was able to induce APC activity toward Securin in these extracts. Addition of $p31^{comet}$ to control- as well as Rassf1A- or Daxx-deficient mitotic extracts (produced from mitotic cells in either nocodazole or taxol block) resulted in equal activation of the APC and subsequent destruction of Securin (Supplementary Figure 5B), whereas addition of recombinant Rassf1 and/or Daxx proteins did not induce activation of the APC (data not shown). Taken together, these results imply that the prolonged mitotic arrest observed upon manipulation of the Rassf1–Daxx complex is not due to an inability to activate the APC, at least *in vitro*. However, as the mechanism(s) of spindle checkpoint silencing/release are poorly understood, we cannot exclude that this complex participates in an upstream event that is not recapitulated in our *in vitro* settings.

Daxx- and Rassf1-dependent tumor response to taxol

Next, we sought to understand the importance of Daxx and Rassf1A in tumor response to taxol using neoplasm generated by a xenograft system. Taxane-based therapy is one of treatment options in head and neck cancer (De Mulder, 1999); therefore, we assessed the antineoplastic activity of taxol exerted on tumors generated from control-, Daxx- or Rassf1A-depleted HEp2 larynx carcinoma cells. By comparing the daily changes in tumor volume (beginning of treatment at approximately 150 mm^3 of tumor) between taxol- and vehicle-treated groups, we could determine regressions in tumor growth. As human tumor xenografts were administered taxol, response of control neoplasms compared with vehicle was markedly sharper owing to the sudden drop in volume even after the first injection of drug. The regression trend was observed further after the 2nd–5th drug administration from days 4 to 11 (Figure 6b). This drug response, in contrast, was reduced in Daxx- or Rassf1A-depleted xenografts as the sizes of taxol-treated tumors in these groups closely followed that of vehicle-administered tumors. The residual tumor size (calculated as a ratio of sizes between taxol- and vehicle-injected tumors at the end of experiment) of Daxx- and Rassf1A-depleted tumors after five administrations of taxol averaged to be 0.65 and 0.66, respectively, whereas the residual size of control-depleted tumors was much smaller at 0.27 (Figure 6a). We concluded that tumors generated from Daxx- and Rassf1A-depleted cells had reduced response rate to taxol administration compared with control-depleted tumors.

We reasoned that the differential taxol response of these tumor groups may, in part, be linked to the cellular outcomes as documented previously (Lindsay *et al*., 2007): taxol-resistant cells arrest in a prolonged mitotic state with sustained cyclin B protein levels and continue cell division upon drug decay, whereas non-resistant cells exit mitosis forming micronucleated cells incapable of entering next cycle. To address this possibility, we analyzed cellular morphology at tumor xenografts sections. Based on DNA staining, cells were categorized as (1) interphase, (2) mitosis, (3) apoptosis and (4) micronuclei (Lindsay *et al*., 2007). In control shRNA xenografts, we observed an increased number of micronucleated cells (indication of taxol response) after

a

Xenograft	End Tumor Size: Vehicle (A)	End Tumor Size: Paclitaxel (B)	Residual Tumor Size (B/A)	N (Animals) Control/ Paclitaxel (Total)
Control shRNA	5.87	1.61	0.27	8/14 (22)
Daxx shRNA	6.23	4.02	0.65	10/15 (25)
Rassf1A shRNA	4.98	3.26	0.66	15/15 (30)

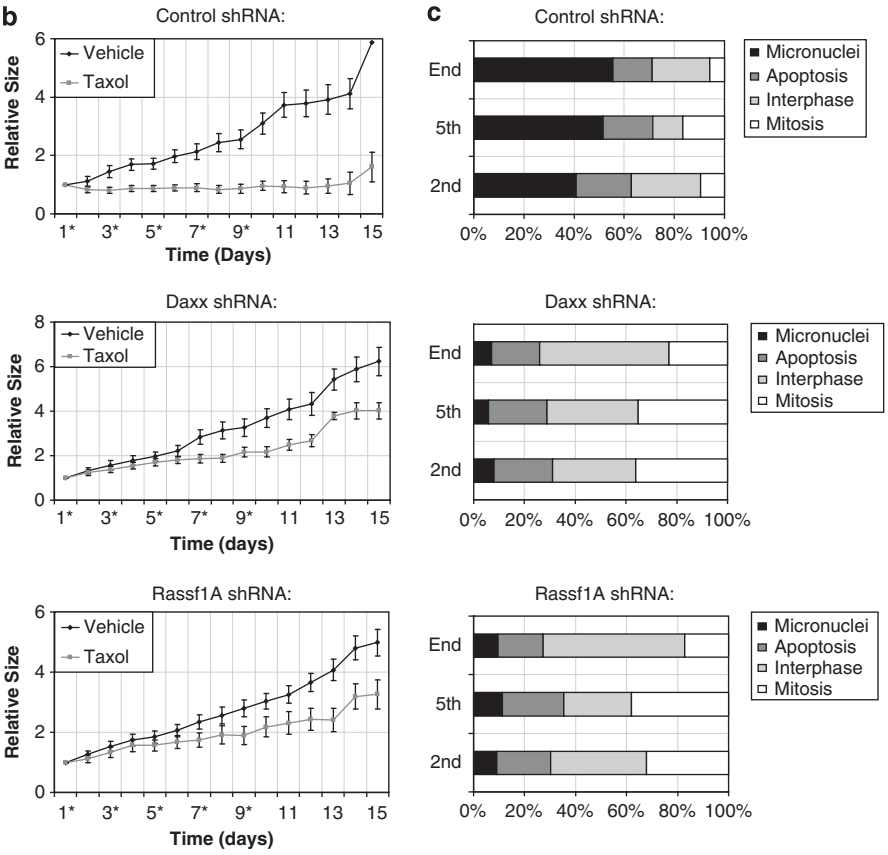

Figure 6 Depletion of Daxx or Rassf1 increases resistance of experimental tumors to taxol. Control-, Daxx- or Rassf1A-depleted tumors derived from injection of HEp2 cells into Nu/Nu mice were treated with vehicle or 20 mg/kg taxol. (**a**) Table summarizing important statistical data generated from tumors exposed to vehicle or taxol regimens. Relative tumor sizes for vehicle- (**a**) or taxol-treated tumors (**b**) were recorded at the end of treatment and the relative residual tumor volumes were calculated by dividing the values from (**b**) over (**a**). (**b**) Graphs charting the changes in relative tumor size of control-, Daxx- or Rassf1A-depleted xenografts exposed to vehicle or taxol. Asterisks at day number (*x* axis) denote the time of injection of vehicle or taxol (days 1, 3, 5, 7 and 9). Note discrepancy in tumor growth in vehicle- and taxol-treated tumors in control shRNA groups, whereas the rate of growth in Daxx- and Rassf1A-shRNA groups exposed to taxol have reduced response. (**c**) Treatment response at cellular level. Tumor xenografts were extracted 24 h following the 2nd or 5th taxol injection or at the end of experiment (day 15) and cellular response was analyzed based on the appearance of chromatin (stained for DNA) by light microscopy and characterized as (1) interphase, (2) mitotic, (3) micronucleated and (4) apoptotic as described previously (Lindsay *et al*., 2007). Control xenografts exhibited an increased number of micronucleated cells (indication of taxol response), whereas Daxx- and Rassf1A-depleted xenografts show increased numbers of mitotic and interphase cells (indication of taxol resistance and continuous proliferation) and correspondingly less micronuclei; number apoptotic cells is similar in all groups.

2nd and 5th injections of taxol, elevating to 50% at the end of treatment. In contrast, the number of interphase and mitotic cells (indication of taxol resistance) in Daxx- and Rassf1-depleted xenografts remained high, whereas that of micronuclei were low (<10% at the end of treatment), suggesting that cells keep cycling (Figure 6c). Occurrence of apoptotic cells was similar across all xenografts and increased marginally upon taxol exposure. Thus, in current experimental settings, depletion of Daxx and Rassf1 elevated resistance of experimental tumors to taxol treatment, with majority of cells continuously cycling—whereas tumors derived from control-depleted cells formed micronuclei and thus stop proliferation.

Daxx levels have reverse correlation with taxane chemotherapy response in breast cancer patients

To address the clinical ramifications of Daxx regulation of taxane sensitivity, 23 women with locally advanced HER-2 non-amplified breast cancer who were treated with standard taxane- and anthracycline-based neoadjuvant chemotherapy at H Lee Moffitt Cancer Center were identified for this study. Patients were classified as either responders or non-responders based on the

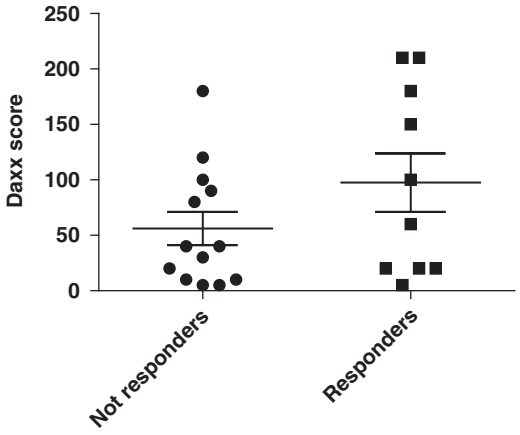

Figure 7 Daxx levels have reverse correlation with taxane chemotherapy response in breast cancer patients. In all, 23 women with breast cancer who were treated with standard taxane- and anthracycline-based neoadjuvant chemotherapy were classified as either responders (up to 75% reduction of tumor size; 10 patients) or non-responders (<75% reduction of tumor size; 13 patients). Daxx score was calculated based on the Daxx immunohistochemistry staining intensity multiplied by the percent of staining cells. Comparison of pretreatment samples between the responders and non-responders was performed using an independent sample *t*-test. Responders to therapy had a higher mean Daxx score compared with non-responders ($P=0.06$).

clinical response measured, with the longest diameter by physical examination performed by the treating physician at the time of encounter, with responders experiencing >75% reduction. Daxx score was calculated based on the Daxx immunohistochemistry staining intensity multiplied by the percent of staining cells. Based on the above definition of response, 10 patients were classified as responders and 13 as non-responders. Comparison of pretreatment samples between the responders and non-responders was performed using an independent sample *t*-test. Responders to therapy had a higher mean Daxx score compared with non-responders (Figure 7; $P=0.06$). These data suggested that Daxx score could predict the response to neoadjuvant taxane- and anthracycline-based chemotherapy. The small sample size and the retrospective nature of the study are the main limitation of this finding that will be further validated in a future prospective study.

Discussion

Taxane chemotherapy is considered among the most responsive treatment options for many cancer patients, either alone or as adjuvant in combination with anthracyclines (O'Shaughnessy, 2005). Nevertheless, large numbers of patients are resistant or become resistant to taxane therapy during treatment. The response rate of docetaxel is ~50% even after the first-line chemotherapy administration and decreases to 20–30% by second- or third-line administration (Bonneterre *et al*., 1999; Crown *et al*., 2004). Thus, development of new genetic prognostic factors and in-depth understanding of drug activity on both cellular and organism levels are needed for optimization of adjuvant therapy and proper patient stratification. Numerous studies have been carried out to determine a genomic profile that could be predictive to taxane treatment (Chang *et al*., 2003, 2005; Miyoshi *et al*., 2004; Iwao-Koizumi *et al*., 2005; Mauriac *et al*., 2005), whereas alternative approaches have sought to understand selective resistance to taxanes to decipher mechanisms that regulate responses (Hari *et al*., 2003a, b; Wang and Cabral, 2005). Inactivation of mitotic proteins can contribute to the selective response of taxane treatment *in vivo* (Wassmann and Benezra, 2001). Divergent response to taxol exposure is usually seen in cells deficient of mitotic checkpoint proteins or other regulators of cell division. To date, loss of function of the majority of mitotic proteins, including Mad1, Mad2, Bub1 and BubR1, among others, has shown enhanced response to taxol in cell culture conditions, implying increased output of micronucleation instead of mitotic arrest (Carvalho *et al*., 2003; Lens *et al*., 2003; Lee *et al*., 2004). Hence, identification of factors, which increase drug resistance upon inactivation, is largely incomplete or uncharacterized.

To this end, Daxx was verified as a novel regulator of taxol response in cell culture conditions, animal models and primary human tumor specimens. Human breast cancer cells and larynx carcinoma HEp2 cells with experimentally modified levels of Daxx show reduced responses to taxol as described previously (Lindsay *et al*., 2007). A mouse xenograft system also recapitulates our initial findings, becoming the first indication that Daxx and its interaction partner Rassf1 could be important for the fate of tumors exposed to taxane-based chemotherapy (Figures 6a and b). We also found that control groups displayed an increased amount of micronucleation upon taxol treatment, which may account for the rapid loss of xenografts tumor volume observed in these regimental settings (Figure 6c). In contrast, Daxx- and Rassf1A-depleted tumors displayed increased mitotic and interphase index (Figure 6c), indicating that cells were capable of maintaining mitotic block via elevated cyclin B stability (Figure 4c) and continue proliferation after taxol decay that happens fast in nude mice (Kubota *et al*., 1997). Thus, mitotic cells from Daxx- and Rassf1A-depleted tumors can potentially re-enter G1 after drug decay, suggesting a working model for how cells or tumors devoid of either of these protein targets can survive chemotherapy treatment and proliferate (Model in Supplementary Figure 6).

The nature of Daxx function in cells is largely attributed to the regulation of apoptosis or transcription. Although this functionality is debatable in many circumstances, the prevailing idea of the role of Daxx is that of a modulator or adapter of many cellular functions, which are critical to cell vitality (Lindsay *et al*., 2008). Indeed, Daxx has been found critical and necessary for embryonic development in mice as $Daxx^{-/-}$ embryos exhibit extensive apoptosis and lethality by E11.5 (Michaelson *et al*., 1999b; Ishov *et al*., 2004). Many Daxx-interacting proteins have also been described, including the interaction between Daxx and Rassf1C (Kitagawa *et al*., 2006; Song *et al*.,

2008). We further characterized this interaction by analyzing the dynamics of cell cycle distribution of Daxx/Rassf1C. Rassf1C (endogenous or transiently expressed; Figures 2a–d) is exclusively cytoplasmic-associated protein and does not reside at PML NBs during interphase, as previously suggested by Kitagawa *et al*. (2006). Moreover, cytoplasmic localization of Rassf1 was unaffected by the presence or absence of Daxx (Figure 2a). In light of these findings, it is difficult to explain the suggested role of Daxx/Rassf1C interaction in Fas-induced apoptosis (Kitagawa *et al*., 2006). We showed that Rassf1C is able to bind Daxx by its unique amino-terminal region (I, Figure 3 and Supplementary Figure 3B, top panel). We also show that Rassf1A and Rassf1C, the two major isoforms of Rassf1 in cells, interact with each other and with Daxx through a common region in their carboxyl termini by *in vitro* pull-down assay (Figure 3 and Supplementary Figure 3).

Rassf1A has been implicated as a mitotic regulator and has been shown to interact with several important mitotic-related proteins, including Aurora A (Rong *et al*., 2007) and Cdc20 (Song *et al*., 2004), although the latter is debatable (Liu *et al*., 2007). These findings together with out data indicate that Rassf1A has a pleiotropic effect during mitosis. This may justify the elevated accumulation of cyclin B observed upon depletion of Rassf1A and taxol exposure (Figure 4c).

The interaction partners of Rassf1C have until now been limited to Daxx, BetaTrCP and IGFBP-5 (Amaar *et al*., 2005; Kitagawa *et al*., 2006; Estrabaud *et al*., 2007), with the cellular functions of Rassf1C, comparatively, being much less studied. As Rassf1A and Rassf1C have many seemingly unrelated interaction partners, the implications of a Rassf1A–Rassf1C interaction via common protein region suggests a converging point of cellular networks and pathways that may have otherwise been unlinked. It is possible that Daxx, Rassf1A and Rassf1C may form three-party functional mitotic complex, where Rassf1C may, at least in some cases, serve as a functional 'bridge' between Daxx and Rassf1A as overexpressing a construct with the Daxx-interacting amino-terminal region of Rassf1C (Figure 5) effectively recapitulates taxol resistance phenotypes seen in Daxx- and Rassf1A-depleted cells (Figure 4b) and xenograft models (Figure 6).

In addition to function in taxol response, we also report an unexpected role of Daxx in the regulation of mitosis. In the absence of Daxx, the duration of prophase and the prometaphase/metaphase transition is altered (Table 1). Indeed, the stability of cyclin B protein is changed in the absence of Daxx as well (Figure 1b). This may suggest that the activity of E3 ubiquitin ligase APC is altered in the absence of Daxx. We attempted to study the role of Daxx and Rassf1 as direct regulators of APC using an *in vitro* assay, but the results were undistinguishable (Supplementary Figure 5), suggesting that cellular *in vivo* mitotic environment is necessary for proper execution of Daxx/Rassf1 function in mitosis. Differential degradation of cyclin B in Daxx-depleted cells could also be due to mis-regulation of cyclin B on a different operational level, namely, the alteration in stability of the APC activator Cdc20 (Nilsson *et al*., 2008). However, we found no differences in and accumulation of Cdc20 as well as Cdc27 and Mad2 (Supplementary Figure 4A). Our results indicate that upon Daxx or Rassf1 depletion and taxane exposure both dynamics of degradation and/or accumulation of cyclin B levels are affected. To date, we cannot explain this phenomenon, although it suggests that Daxx- or Rassf1-mediated regulation of cyclin B may occur at multiple levels. Thus, the detailed mechanism and players underlying the functions of Daxx in mitotic progression remain largely unknown and future studies aimed at unraveling cell cycle-specific roles of Daxx are required.

Evidences presented in this study suggest that Daxx and Rassf1 are triggers for cellular taxol sensitivity, which together with the recently reported function of Daxx in the transcription repression of the prometastatic tyrosine kinase receptor c-met (Morozov *et al*., 2008) may further uncover Daxx function in tumor progression. In the future, Daxx and Rassf1 may serve as useful molecular markers for proper selection of cancer patients for taxane chemotherapy. To achieve this goal, clinical studies additional to that presented here (Figure 7) will be required to examine the status of Daxx and Rassf1 expression in tumors before and after taxane treatment, as well as studies in patients with an established history of taxane resistance. Daxx expression vary in breast cancer cell lines (Lindsay *et al*., 2007), but the mechanism of Daxx downregulation has largely been unstudied. Rassf1A expression in cancer cell lines, conversely, has been extensively covered and shown to be downregulated in a majority of cases (Agathanggelou *et al*., 2005). Our studies have established new roles for Daxx in cell cycle progression—the importance of which may be intensified because of its function as a trigger for taxol sensitization in combination with Rassf1—which adds to our understanding of mechanisms linking cell division, chemotherapy response and cancer progression.

Materials and methods

Biochemical fractionation

HEp2 cells were separated into nuclear and cytosolic fractions using a biochemical fractionation method described by Lindsay *et al*. (2009).

Cell culture

HEp2 cells and primary mouse embryonic fibroblasts (Ishov *et al*., 2004) were cultured in Dulbecco's modified Eagle's medium supplemented with 10% fetal bovine serum, 2 mM glutamine and 100 U/ml penicillin and 100 μg/ml streptomycin (Gibco BRL, Carlsbad, CA, USA) and grown in a humidified 5% CO_2 incubator. Taxol (Paclitaxel; Sigma, St Louis, MO, USA; 100 μM in dimethyl sulfoxide) was used at a final concentration of 10 nM. Thymidine (Sigma) was dissolved in 1 N NaOH for 1 M stock and used at a final concentration of 2 mM.

Cell cycle synchronization
HEp2 cells were synchronized using a double thymidine block protocol as described in (Lindsay *et al*., 2007). For taxol studies, 10 nM taxol was added 6 h after release of cells from second thymidine block; at this time point, up to 95% of cells were accumulated in the G2 phase by fluorescence-activated cell sorting analysis.

Colony formation assay
Cells exposed to control or 10 nM taxol were originally plated on 3.5 cm dishes (Corning Incorporated, Lowell, MA, USA) for treatment. Following exposure, cells were trypsinized and re-plated (in triplicates) at 1:1000 dilution on six-well plates (Corning Incorporated) for colony formation analysis. At 5–7 days afterwards, colonies were stained with crystal violet and counted.

Immunofluorescence
Immunofluorescence analysis was completed on cells grown overnight on coverslips in 24-well plates (Costar). Briefly, cells were fixed using 1% formaldehyde or ice-cold methanol (for analysis of microtubules). Following fixation, cells were permeabilized with 0.4% Triton X-100 (formaldehyde-fixed cells only). Cells were incubated for 1 h with the following primary antibodies: Daxx rabbit (Santa Cruz Biotechnology, Santa Cruz, CA, USA), Daxx 5.14 monoclonal (Ishov *et al*., 2004), PML 14 rabbit (Ishov *et al*., 1999), Rassf1C mouse polyclonal (UT Southwestern Medical Center, Dallas, TX, USA), Rassf1 rabbit (gift from Dr Dae Sik Lim, Korea Advanced Institute for Science and Technology, Daejeon, South Korea) and α-tubulin (Sigma). Cells were washed in phosphate-buffered saline (PBS) and incubated with appropriate fluorescein isothiocyanate- or Texas Red-conjugated secondary antibodies (Vector Laboratories, Burlingame, CA, USA; all diluted 1:300), stained with Hoechst 33342 (Sigma) for DNA visualization and mounted on slides with Fluoromount G (Southern Biotech, Birmingham, AL, USA). Images were analyzed using Leica TCS SP5 confocal microscope.

Immunohistochemistry
For this study, 23 women were identified with locally advanced HER-2 non-amplified breast cancer who were treated with standard taxane/anthracycline-based neoadjuvant chemotherapy at H Lee Moffitt Cancer Center. Initial core biopsy was performed for the diagnosis and all patients underwent neoadjuvant chemotherapy, followed by definitive surgery with either lumpectomy or mastectomy and axillary lymph node dissection. Two patients had invasive lobular carcinoma, one patient papillary carcinoma, whereas the remainder had invasive ductal carcinoma. Four tumors were hormone receptor negative and 19 tumors were hormone receptor positive. Tissue blocks were obtained from initial biopsy (before neoadjuvant chemotherapy) to perform immunohistochemical staining for Daxx. Slides were de-paraffinized with xylene and re-hydrated through decreasing concentrations of ethanol to water, including an intermediary step to quench endogenous peroxidase activity (3% hydrogen peroxide in methanol). For heat-induced antigen retrieval, sections were heated in a water bath at 95 °C while submerged in Trilogy buffer (Cell Marque, Hot Springs, AR, USA) for 25 min and afterwards incubated with a universal protein blocker Sniper (Biocare Medical, Walnut Creek, CA, USA) for 15 min at room temperature (RT). Monoclonal mouse anti-Daxx 5.14 was added at RT. Mach 2 goat anti-mouse-horse radish peroxidase conjugate (Biocare Medical, Walnut Creek, CA, USA) was then added for 30 min RT. Detection of Daxx was achieved by incubating slides in 3′3′-diaminobenzidine (Biocare Medical) for 15 min at RT. Slides were counterstained with hematoxylin (Vector Laboratories Inc., Burlingame, CA, USA) for 10 s and mounted with Cytoseal XYL (Richard-Allen Scientific, Kalamazoo, MI, USA). Slides were analyzed using Leica DM2000 microscope and pictures were taken using Leica DFC480 CCD camera with the Leica FireCam 1.7.1 software. For each specimen, at least one thousand cells were examined for Daxx expression, and the number of cells with an evident signal were recorded and categorized by the intensity of staining (0 for undetectable, 5 for highest) of Daxx multiplied by the percent of staining cells (Daxx score).

Time-lapse microscopy
Time-lapse imaging of cells was performed according to Meraldi *et al*. (2004). Briefly, control- and Daxx-depleted HEp2 cells were stably transfected with GFP-histone H2B (gift from Dr Duane Compton, Dartmouth, Hanover, NH, USA) and analyzed by Leica TCS SP5 confocal microscope equipped with environmental chamber; images were taken every 2 min. Mitotic stages were determined by three hallmark events including (1) first indication of chromatin condensation marked as late G2/prophase transition ($T=0$); (2) invagination of the nucleus marking the prophase/prometaphase transition; and (3) beginning of chromosome segregation marking the metaphase/anaphase transition. Three experiments were completed for each shRNA group with an average of 20–30 cells per experiment.

Yeast two-hybrid screen
mDaxx wild type was cloned in pGBDC1-Trp1 and transformed in PJ69-4A MATa and tested for self-activation. Screening for Daxx interaction partners was carried out using pre-transformedi (Y187 yeast strain, MATa) cDNA library from E11 embryos (library in pACT2 Leu2; Clontech, Mountain View, CA, USA; no. MY4012AH). Sequence analysis of two strong interaction clones from -His-Leu-Trp plates revealed homology with amino acids 5–270 and 30–270 of mouse Rassf1C. Retransformation and β-gal assay confirmed the specificity of this interaction in yeast.

In vitro *pull-down assay*
Daxx constructs were cloned into pGEX-2T or pGEX-4T3 (Invitrogen, Carlsbad, CA, USA). Rassf1 construct were generated in pQE-30 (Qiagen, Valencia, CA, USA) or pMAL-c2x vectors (New England BioLabs, Ipswich, MA, USA). Constructs were then transformed into a Rosetta strain of *Escherichia coli*. Protein expression was induced using 50 μM isopropyl-β-D-thiogalactopyranoside (Fisher BioReagents, Fair Lawn, NJ, USA) (pGEX-4T3 constructs), 0.1 mM isopropyl-β-D-thiogalactopyranoside (pQE-30 constructs) or 0.3 mM isopropyl-β-D-thiogalactopyranoside (pMAL constructs) at RT for 3 h (pGEX and pMAL) or 18 °C overnight (pQE-30). Cells were lysed using buffer consisting of 0.1% Triton X-100, 200 μM phenylmethylsulfonyl fluoride (Calbiochem, EMD Chemicals, Gibbstown, NJ, USA), 1 μg/ml aprotinin (Sigma), 1 μM leupeptin (Sigma), 1 μM pepstatin (Sigma) and 10 mM 2-mercaptoethanol (Sigma) in Tris-buffered saline. A glutathione-*S*-transferase- and 6 × -His pull-down kit (Pierce Biotechnology, Rockford, IL, USA) was then used to determine binding capability as per the manufacturer's instructions. Maltose-binding protein and derivative fusion proteins were purified following instructions for pMAL protein fusion and purification system (New England BioLabs). Protein samples were analyzed on 4–20%

sodium dodecyl sulfate–polyacrylamide gel electrophoresis gels (Bio-Rad, Hercules, CA, USA).

Mouse xenografts
HEp2 xenografts were generated in Nu/Nu mice by subcutaneous injection of 5×10^6 HEp2 cells containing a 1:1 mixture of matrigel (BD Biosciences, San Jose, CA, USA)/Dulbecco's modified Eagle's medium suspension. Tumors were monitored daily and grown to a volume of approximately 150 mm^3 (days 7–9 after cell injection) before drug treatment. Vehicle (1 part of 1:1 solution of 50% EtOH/Cremaphor EL (Sigma) to 10 parts of PBS) or 20 mg/kg taxol (LC Laboratories, Woburn, MA, USA; Paclitaxel stock = 25 mg/ml dissolved in EtOH/Cremaphor EL) was injected intraperitoneally every second day for a total of five injections. Up to 15 animals were used for each experimental group. Tumor volume was measured by calipers and calculated on a daily basis using the formula $V = (1/6) \times \pi a(b)^2$, where a and b are the measured length and width (millimeters) of the tumor, respectively. Increases or reductions in tumor size were determined according to the relative initial tumor size beginning on day 1 of injection. Experiment was terminated at day 15 of first drug injection or when tumor volume reaches 1000 mm^3.

shRNA
HEp2 cells were transduced with recombinant lentivirus supernatants encoding hairpin siRNA for hDaxx, hRassf1A and control expression constructs in the presence of 4 μg/ml polybrene. The lentiviral expression system was provided by Peter M Chumakov (Lerner Research Institute, Cleveland, OH, USA; Sablina *et al*. (2005)). This lentiviral system comprises a targeting envelope expression vector pCMV-VSV-G, a generic packaging expression vector pCMV-deltaR8.2 and the expression cassette for custom siRNA pLSL-GFP that contains a minimal histone H4 promoter that drives transcription of a *GFP* gene allowing fluorescent cell sorting. Candidate siRNAs for Daxx and Rassf1A were designed according to the Dharmacon si*DESIGN* algorithm (http://www.dharmacon.com/sidesign/). Anti-Daxx siRNA 1 was targeted against base pairs 1552–1570 of hDaxx (CTAC AGATCTCCAATGAAA); anti-Daxx siRNA 2 was targeted against base pairs 100–118 of hDaxx (GATGAAGCAGCTG CTCAGC); anti-Rassf1A si1 was targeted against base pairs 282–300 of AF132675 (hRassf1A) (TGCGCGCATTGCAAG TTCA); control siRNA was directed against base pairs 1262–1284 of SETDB1 (TCCTCTTTCTTATCCTCGTATGT).

Western blot analysis
Protein samples were separated by 4–20% sodium dodecyl sulfate–polyacrylamide gel electrophoresis (Bio-Rad), transferred to nitrocellulose membranes (Whatman, Dassel, Germany) and blocked with 3% non-fat milk/PBS, 0.1% Tween (PBST). Primary antibodies to Daxx 677 rabbit (in house produced), Rassf1A (ab23950; Abcam, Cambridge, MA, USA), actin (A 5316; Sigma), maltose-binding protein (E8032S; New England BioLabs), glutathione-*S*-transferase (G 1160; Sigma), His-G (46-1008; Invitrogen) cyclin B1 (SC-245; Santa Cruz), Cdc20 (SC-8358; Santa Cruz), Cdc27 (SC-9972; Santa Cruz), Mad2 (SC-47747; Santa Cruz), GFP (Living Colors Av peptide Antibody: 632377; Clontech), Rassf1 (gift from Dr Gerd Pfeifer) or HP1-α (gift from Dr Frank Rauscher) were diluted in 3% milk/PBST and incubated overnight at 4 °C. Membranes were then washed 3 × with PBST for 1 h at RT with appropriate secondary antibody (Chemicon; all 1:2500). Membranes were then washed with PBST and exposed using ECL reagent (Amersham, GE Healthcare, Pittsburg, PA, USA). Densitometry analysis of cyclin B and actin western blots was performed using the Quantity One software from Bio-Rad (Hercules, CA, USA).

APC assay
Cellular pellets were resuspended in lysis buffer (20 mM Tris–HCl, pH 7.2, 2 mM dithiothreitol, 0.25 mM EDTA, 5 mM KCl, 5 mM $MgCl_2$) on ice and subjected to 1500 psi N_2 in a nitrogen disruption chamber. The lysate was spun for 15 min at 15 000 *g*. Supernatants were divided into single-use aliquots and flash frozen in N_2. For assays, extracts, on ice, were supplemented with an energy-regenerating system (30 U/ml rabbit creatine phosphokinase type I, 7.5 mM creatine phosphate, 1 mM ATP, 1 mM $MgCl_2$, 0.1 mM EGTA), non-destructible cyclin B and cycloheximide. Proteins were then added in a final volume of 14 ml. ^{35}S-labeled substrate (1 ml) was added; aliquots were made and shifted to 30 °C. Samples were quenched at the indicated times by the addition of sample buffer, resolved by sodium dodecyl sulfate–polyacrylamide gel electrophoresis and imaged using a Typhoon PhosphorImager (GE Healthcare).

Conflict of interest

The authors declare no conflicts of interest.

Acknowledgements

We thank Dr Gerd Pfeifer, Beckman Research Institute, for the generous gift of anti-Rassf1 antibodies and Dr Frank Rauscher, The Wistar Institute, for HP1 antibodies. This work was supported by NIH/NCI R01 CA127378-01A1 for CRL, SG, VMM and AMI, by the Canadian Cancer Society (017308) for EE and LPM. NMR spectroscopy support was provided by the Canadian Institutes for Health Research (CIHR), the Canadian Foundation for Innovation (CFI), the British Columbia Knowledge Development Fund (BCKDF), the UBC Blusson Fund and the Michael Smith Foundation for Health Research (MSFHR).

References

Aapro MS. (2001). Neoadjuvant therapy in breast cancer: can we define its role? *Oncologist* **6**(Suppl 3): 36–39.

Agathanggelou A, Cooper WN, Latif F. (2005). Role of the Ras-association domain family 1 tumor suppressor gene in human cancers. *Cancer Res* **65**: 3497–3508.

Amaar YG, Baylink DJ, Mohan S. (2005). Ras-association domain family 1 protein, RASSF1C, is an IGFBP-5 binding partner and a potential regulator of osteoblast cell proliferation. *J Bone Miner Res* **20**: 1430–1439.

Bonneterre J, Spielman M, Guastalla JP, Marty M, Viens P, Chollet P *et al*. (1999). Efficacy and safety of docetaxel (Taxotere) in heavily pretreated advanced breast cancer patients: the French compassionate use programme experience. *Eur J Cancer* **35**: 1431–1439.

Brito DA, Rieder CL. (2006). Mitotic checkpoint slippage in humans occurs via cyclin B destruction in the presence of an active checkpoint. *Curr Biol* **16**: 1194–1200.

Carvalho A, Carmena M, Sambade C, Earnshaw WC, Wheatley SP. (2003). Survivin is required for stable checkpoint activation in taxol-treated HeLa cells. *J Cell Sci* **116**: 2987–2998.

Chabalier C, Lamare C, Racca C, Privat M, Valette A, Larminat F. (2006). BRCA1 downregulation leads to premature inactivation of spindle checkpoint and confers paclitaxel resistance. *Cell Cycle* **5**: 1001–1007.

Chang JC, Wooten EC, Tsimelzon A, Hilsenbeck SG, Gutierrez MC, Elledge R *et al*. (2003). Gene expression profiling for the prediction of therapeutic response to docetaxel in patients with breast cancer. *Lancet* **362**: 362–369.

Chang JC, Wooten EC, Tsimelzon A, Hilsenbeck SG, Gutierrez MC, Tham YL *et al*. (2005). Patterns of resistance and incomplete response to docetaxel by gene expression profiling in breast cancer patients. *J Clin Oncol* **23**: 1169–1177.

Crown J, O'Leary M, Ooi WS. (2004). Docetaxel and paclitaxel in the treatment of breast cancer: a review of clinical experience. *Oncologist* **9**(Suppl 2): 24–32.

Dallol A, Agathanggelou A, Fenton SL, Ahmed-Choudhury J, Hesson L, Vos MD *et al*. (2004). RASSF1A interacts with microtubule-associated proteins and modulates microtubule dynamics. *Cancer Res* **64**: 4112–4116.

De Mulder PH. (1999). The chemotherapy of head and neck cancer. *Acta Otorhinolaryngol Belg* **53**: 247–252.

Escobar-Cabrera E, Lau DK, Giovinazzi S, Ishov AM, McIntosh LP. (2010). Structural characterization of the DAXX N-terminal helical bundle domain and its complex with Rassf1C. *Structure* **18**: 1642–1653.

Estrabaud E, Lassot I, Blot G, Le Rouzic E, Tanchou V, Quemeneur E *et al*. (2007). RASSF1C, an isoform of the tumor suppressor RASSF1A, promotes the accumulation of beta-catenin by interacting with betaTrCP. *Cancer Res* **67**: 1054–1061.

Hari M, Wang Y, Veeraraghavan S, Cabral F. (2003a). Mutations in alpha- and beta-tubulin that stabilize microtubules and confer resistance to colcemid and vinblastine. *Mol Cancer Ther* **2**: 597–605.

Hari M, Yang H, Zeng C, Canizales M, Cabral F. (2003b). Expression of class III beta-tubulin reduces microtubule assembly and confers resistance to paclitaxel. *Cell Motil Cytoskeleton* **56**: 45–56.

Henderson IC, Berry DA, Demetri GD, Cirrincione CT, Goldstein LJ, Martino S *et al*. (2003). Improved outcomes from adding sequential Paclitaxel but not from escalating Doxorubicin dose in an adjuvant chemotherapy regimen for patients with node-positive primary breast cancer. *J Clin Oncol* **21**: 976–983.

Ishov AM, Sotnikov AG, Negorev D, Vladimirova OV, Neff N, Kamitani T *et al*. (1999). PML is critical for ND10 formation and recruits the PML-interacting protein daxx to this nuclear structure when modified by SUMO-1. *J Cell Biol* **147**: 221–234.

Ishov AM, Vladimirova OV, Maul GG. (2004). Heterochromatin and ND10 are cell-cycle regulated and phosphorylation-dependent alternate nuclear sites of the transcription repressor Daxx and SWI/SNF protein ATRX. *J Cell Sci* **117**: 3807–3820.

Iwao-Koizumi K, Matoba R, Ueno N, Kim SJ, Ando A, Miyoshi Y *et al*. (2005). Prediction of docetaxel response in human breast cancer by gene expression profiling. *J Clin Oncol* **23**: 422–431.

Kitagawa D, Kajiho H, Negishi T, Ura S, Watanabe T, Wada T *et al*. (2006). Release of RASSF1C from the nucleus by Daxx degradation links DNA damage and SAPK/JNK activation. *EMBO J* **25**: 3286–3297.

Kubota T, Matsuzaki SW, Hoshiya Y, Watanabe M, Kitajima M, Asanuma F *et al*. (1997). Antitumor activity of paclitaxel against human breast carcinoma xenografts serially transplanted into nude mice. *J Surg Oncol* **64**: 115–121.

Lee EA, Keutmann MK, Dowling ML, Harris E, Chan G, Kao GD. (2004). Inactivation of the mitotic checkpoint as a determinant of the efficacy of microtubule-targeted drugs in killing human cancer cells. *Mol Cancer Ther* **3**: 661–669.

Lens SM, Wolthuis RM, Klompmaker R, Kauw J, Agami R, Brummelkamp T *et al*. (2003). Survivin is required for a sustained spindle checkpoint arrest in response to lack of tension. *EMBO J* **22**: 2934–2947.

Lindsay CR, Giovinazzi S, Ishov AM. (2009). Daxx is a predominately nuclear protein that does not translocate to the cytoplasm in response to cell stress. *Cell Cycle* **8**: 1544–1551.

Lindsay CR, Morozov VM, Ishov AM. (2008). PML NBs (ND10) and Daxx: from nuclear structure to protein function. *Front Biosci* **13**: 7132–7142.

Lindsay CR, Scholz A, Morozov VM, Ishov AM. (2007). Daxx shortens mitotic arrest caused by paclitaxel. *Cell Cycle* **6**: 1200–1204.

Liu L, Baier K, Dammann R, Pfeifer GP. (2007). The tumor suppressor RASSF1A does not interact with Cdc20, an activator of the anaphase-promoting complex. *Cell Cycle* **6**: 1663–1665.

Liu L, Tommasi S, Lee DH, Dammann R, Pfeifer GP. (2003). Control of microtubule stability by the RASSF1A tumor suppressor. *Oncogene* **22**: 8125–8136.

Mantel C, Guo Y, Lee MR, Han MK, Rhorabough S, Kim KS *et al*. (2008). Cells enter a unique intermediate 4*N* stage, not 4*N*-G1, after aborted mitosis. *Cell Cycle* **7**: 484–492.

Mauriac L, Debled M, MacGrogan G. (2005). When will more useful predictive factors be ready for use? *Breast* **14**: 617–623.

Meraldi P, Draviam VM, Sorger PK. (2004). Timing and checkpoints in the regulation of mitotic progression. *Dev Cell* **7**: 45–60.

Michaelson JS. (2000). The Daxx enigma. *Apoptosis* **5**: 217–220.

Michaelson JS, Bader D, Kuo F, Kozak C, Leder P. (1999a). Loss of Daxx, a promiscuously interacting protein, results in extensive apoptosis in early mouse development. *Genes Dev* **13**: 1918–1923.

Michaelson JS, Bader D, Kuo F, Kozak C, Leder P. (1999b). Loss of daxx, a promiscuously interacting protein, results in extensive apoptosis in early mouse development [In Process Citation]. *Genes Dev* **13**: 1918–1923.

Miyoshi Y, Kim SJ, Akazawa K, Kamigaki S, Ueda S, Yanagisawa T *et al*. (2004). Down-regulation of intratumoral aromatase messenger RNA levels by docetaxel in human breast cancers. *Clin Cancer Res* **10**: 8163–8169.

Morozov VM, Massoll NA, Vladimirova OV, Maul GG, Ishov AM. (2008). Regulation of c-met expression by transcription repressor Daxx. *Oncogene* **27**: 2177–2186.

Niikura Y, Dixit A, Scott R, Perkins G, Kitagawa K. (2007). BUB1 mediation of caspase-independent mitotic death determines cell fate. *J Cell Biol* **178**: 283–296.

Nilsson J, Yekezare M, Minshull J, Pines J. (2008). The APC/C maintains the spindle assembly checkpoint by targeting Cdc20 for destruction. *Nat Cell Biol* **10**: 1411–1420.

O'Shaughnessy J. (2005). Extending survival with chemotherapy in metastatic breast cancer. *Oncologist* **10**(Suppl 3): 20–29.

Ravdin P, Erban J, Overmoyer B. (2003). Phase III comparison of docetaxel and paclitaxel in patients with metastatic breast cancer (abstract). *Eur J Cancer* (Suppl 1): 32.

Rong R, Jiang LY, Sheikh MS, Huang Y. (2007). Mitotic kinase Aurora-A phosphorylates RASSF1A and modulates RASSF1A-mediated microtubule interaction and M-phase cell cycle regulation. *Oncogene* **26**: 7700–7708.

Rong R, Jin W, Zhang J, Sheikh MS, Huang Y. (2004). Tumor suppressor RASSF1A is a microtubule-binding protein that stabilizes microtubules and induces G2/M arrest. *Oncogene* **23**: 8216–8230.

Sablina AA, Budanov AV, Ilyinskaya GV, Agapova LS, Kravchenko JE, Chumakov PM. (2005). The antioxidant function of the p53 tumor suppressor. *Nat Med* **11**: 1306–1313.

Saffert RT, Kalejta RF. (2008). Promyelocytic leukemia-nuclear body proteins: herpesvirus enemies, accomplices, or both? *Fut Virol* **3**: 265–277.

Salomoni P, Khelifi AF. (2006). Daxx: death or survival protein? *Trends Cell Biol* **16**: 97–104.

Scolnick DM, Halazonetis TD. (2000). Chfr defines a mitotic stress checkpoint that delays entry into metaphase. *Nature* **406**: 430–435.

Song MS, Song SJ, Ayad NG, Chang JS, Lee JH, Hong HK *et al*. (2004). The tumour suppressor RASSF1A regulates mitosis by inhibiting the APC–Cdc20 complex. *Nat Cell Biol* **6**: 129–137.

Song MS, Song SJ, Kim SY, Oh HJ, Lim DS. (2008). The tumour suppressor RASSF1A promotes MDM2 self-ubiquitination by disrupting the MDM2–DAXX–HAUSP complex. *EMBO J* **27**: 1863–1874.

Sudo T, Nitta M, Saya H, Ueno NT. (2004). Dependence of paclitaxel sensitivity on a functional spindle assembly checkpoint. *Cancer Res* **64**: 2502–2508.

Summers MK, Pan B, Mukhyala K, Jackson PK. (2008). The unique N terminus of the UbcH10 E2 enzyme controls the threshold for APC activation and enhances checkpoint regulation of the APC. *Mol Cell* **31**: 544–556.

Swanton C, Marani M, Pardo O, Warne PH, Kelly G, Sahai E *et al*. (2007). Regulators of mitotic arrest and ceramide metabolism are determinants of sensitivity to paclitaxel and other chemotherapeutic drugs. *Cancer Cell* **11**: 498–512.

Wang Y, Cabral F. (2005). Paclitaxel resistance in cells with reduced beta-tubulin. *Biochim Biophys Acta* **1744**: 245–255.

Wassmann K, Benezra R. (2001). Mitotic checkpoints: from yeast to cancer. *Curr Opin Genet Dev* **11**: 83–90.

Wysong DR, Chakravarty A, Hoar K, Ecsedy JA. (2009). The inhibition of Aurora A abrogates the mitotic delay induced by microtubule perturbing agents. *Cell Cycle* **8**: 876–888.

Xia G, Luo X, Habu T, Rizo J, Matsumoto T, Yu H. (2004). Conformation-specific binding of p31(comet) antagonizes the function of Mad2 in the spindle checkpoint. *EMBO J* **23**: 3133–3143.

Supplementary Information accompanies the paper on the Oncogene website (http://www.nature.com/onc)